Inflammation and insulin resistance induced by *trans*-10, *cis*-12 conjugated linoleic acid depend on intracellular calcium levels in primary cultures of human adipocytes

Arion Kennedy,* Kristina Martinez,* Soonkyu Chung,[†] Kathy LaPoint,* Robin Hopkins,*
Soren F. Schmidt,[§] Kenneth Andersen,[§] Susanne Mandrup,[§] and Michael McIntosh[1],*

Department of Nutrition,* University of North Carolina at Greensboro, Greensboro, NC; Wake Forest University School of Medicine,[†] Winston-Salem, NC; and Department of Biochemistry and Molecular Biology,[§] University of Southern Denmark, Odense, Denmark

Abstract   We previously demonstrated that *trans*-10, *cis*-12 (10,12) conjugated linoleic acid (CLA) induced inflammation and insulin resistance in primary human adipocytes by activating nuclear factor κB (NFκB) and extracellular signal-related kinase (ERK) signaling. In this study, we demonstrated that the initial increase in intracellular calcium ($[Ca^{2+}]_i$) mediated by 10,12 CLA was attenuated by TMB-8, an inhibitor of calcium release from the endoplasmic reticulum (ER), by BAPTA, an intracellular calcium chelator, and by D609, a phospholipase C (PLC) inhibitor. Moreover, BAPTA, TMB-8, and D609 attenuated 10,12 CLA–mediated production of reactive oxygen species (ROS), activation of ERK1/2 and cJun-NH$_2$-terminal kinase (JNK), and induction of inflammatory genes. 10,12 CLA–mediated binding of NFκB to the promoters of interleukin (IL)-8 and cyclooxygenase (COX)-2 and induction of calcium-calmodulin kinase II (CaMKII) β were attenuated by TMB-8. KN-62, a CaMKII inhibitor, also suppressed 10,12 CLA–mediated ROS production and ERK1/2 and JNK activation. Additionally, KN-62 attenuated 10,12 CLA induction of inflammatory and integrated stress response genes, increase in prostaglandin $F_{2\alpha}$, and suppression of peroxisome proliferator activated receptor γ protein levels and insulin-stimulated glucose uptake.▮ These data suggest that 10,12 CLA increases inflammation and insulin resistance in human adipocytes, in part by increasing $[Ca^{2+}]_i$ levels, particularly calcium from the ER.—Kennedy, A., K. Martinez, S. Chung, K. LaPoint, R. Hopkins, S. F. Schmidt, K. Andersen, S. Mandrup, and M. McIntosh. Inflammation and insulin resistance induced by *trans*-10, *cis*-12 conjugated linoleic acid depend on intracellular calcium levels in primary cultures of human adipocytes. *J. Lipid Res.* 2010. **51:** 1906–1917.

Supplementary key words   cell signaling • fatty acid • reactive oxygen species

Obesity and its comorbidities are the most prevalent metabolic diseases in the US, affecting over 30% of the adult population (1). Conjugated linoleic acid (CLA), dienoic isomers of linoleic acid, is one potential treatment for obesity. Animal (2) and human studies (3) have demonstrated that supplementation with *trans*-10, *cis*-12 (10,12) CLA alone or in a mixture with the *cis*-9, *trans*-11 (9,11) isomer reduces body weight and fat deposition. 10,12 CLA has been shown to suppress the mRNA and protein levels of peroxisome proliferator activated receptor γ (PPARγ), the master regulator of adipogenesis, in murine 3T3-L1 adipocytes (4) and cultures of newly differentiated human adipocytes (5).

Our research group has reported that 10,12 CLA, but not 9,11 CLA, inhibited human preadipocyte differentiation (6) and caused delipidation of newly differentiated human adipocytes (5). Isomer-specific delipidation of adipocytes by CLA was due largely to a decrease in adipogenic/lipogenic gene expression, uptake of glucose and fatty acids, and triglyceride (TG) synthesis as opposed to an increase in oxidation (5, 7). Interestingly, 10,12 CLA suppression of glucose and fatty acid uptake was dependent on activation of mitogen-activated protein kinase/extracellular kinase signal-regulated kinase (MEK/ERK) and nuclear factor κB (NFκB) signaling, as well as robust secretion or expression of the proinflammatory cytokines interleukin (IL)-6, IL-8, and tumor necrosis factor (TNF)α (5, 7, 9). Consistent with these in vitro data, CLA supplementation in humans is associated with hyperglycemia, dyslipidemia, insulin resistance, and elevated levels of inflammatory prostaglandins (PG) and cytokines (10–13). However, the upstream mechanism(s) by which 10,12 CLA induces inflammation, insulin resistance, and adipocyte delipidation remain unclear.

One possible upstream mediator of CLA-induced inflammation and insulin resistance is intracellular calcium ($[Ca^{2+}]_i$), which is a vital second messenger for the activation of proteins involved in adipocyte proliferation, differentiation, and metabolism (14). Elevated levels of $[Ca^{2+}]_i$ have been reported to activate NFκB (15–17), ERK1/2 (15, 16, 18), and phospholipase A2 (PLA$_2$) (19, 20), leading to cytokine or PG production. Calmodulin (CaM), a major calcium-dependent protein, plays an important role in inflammation and metabolism. CaM activates a number of protein kinases, such as CaMKI, II, and IV (21, 22). Relevant to this study, CaMKII has been shown to inhibit adipocyte differentiation in response to inflammatory PGs such as PGF$_{2\alpha}$ (23).

On the basis of the critical role of $[Ca^{2+}]_i$ in cell signaling, enzyme activation, and adipocyte differentiation, we hypothesized that $[Ca^{2+}]_i$ is an upstream mediator of 10,12 CLA–induced inflammation and insulin resistance in human adipocytes. In this study, we demonstrated for the first time that CLA increases $[Ca^{2+}]_i$ levels, leading to the production of reactive oxygen species (ROS), NFκB, cJun-NH$_2$-terminal kinase (JNK), ERK1/2, and ultimately, the induction of inflammatory genes and PGs, and insulin resistance in human adipocytes.

MATERIALS AND METHODS

Materials

All cell culture ware were purchased from Fisher Scientific (Norcross, GA). Western lightning Chemiluminescence Substrate was purchased from Perkin Elmer Life Science (Boston, MA). Immunoblotting buffers and precast gels were purchased from Invitrogen (Carlsbad, CA). The polyclonal antibody for anti-glyceraldehyde-3-phosphate dehydrogenase (GAPDH) (sc20357) was obtained from Santa Cruz Biotechnology (Santa Cruz, CA). Anti-phospho (P) (Thr183/185) SAPK/JNK and anti-P (Thr-202/204) and total ERK1/2 antibodies were purchased from Cell Signaling Technologies (Beverly, MA). Hyclone fetal bovine serum (FBS) was purchased from Fisher Scientific. Isomers of CLA (+98% pure) were purchased from Matreya (Pleasant Gap, PA). Dichlorofluorescein (DCF), Fluo-3 acetoxymethyl ester (Fluo-3 AM), 1,2-bis (2-aminophenoxy)ethane-N, N, N′, N′-tetraacetic acid (BAPTA)-AM, and 5,5′,6,6′-tetrachloro-1,1′,3,3′-tetraethylbenzimideazole carbocyanine iodide (JC-1) were purchased from Molecular Probes (Eugene, OR). 8-(N,N-diethylamino)-octyl-3,4,5-trimethoxy-benzoate (TMB-8), thapsigargin, and 1-[N,O-*bis*-(5-Isoquinolinesulfonyl)-N-methyl-L-tyrosyl]4-phenylpiperazine (KN-62) were purchased from Calbiochem-EMD Biosciences, Inc. (La Jolla, CA). Ethylene glycol-bis(β-aminoethylester)-N,N,N′,N′-tetracetic acid (EGTA) was purchased from Sigma Chemical Co. (St. Louis, MO). All other reagents and chemicals were purchased from Sigma Chemical Co. unless otherwise stated.

Culturing of human primary adipocytes

Abdominal white adipose tissue (WAT) was obtained, with consent from the institutional review boards at the University of North Carolina at Greensboro and Moses Cone Memorial Hospital, during abdominoplasty of nondiabetic Caucasian and African American females between the ages of 20 and 50 years with a body mass index ≤ 32.0. Tissue was digested using collagenase; stromal vascular cells were isolated as previously described (5). Cultures containing newly differentiated human adipocytes were treated on day 6–12 of the differentiation program. Each independent experiment was repeated at least twice using a mixture of cells from two or three subjects, unless otherwise indicated.

Culturing of human Simpson-Golabi-Behmel Syndrome cells

Simpson-Golabi-Behmel Syndrome (SGBS) cells were generously provided by Dr. Martin Wabitsch at the University of Ulm, Ulm, Germany. They were grown to confluence in DMEM/Nutrient Mixture F-12 Ham's supplemented with 10% bovine serum, 33 μM biotin, 17 μM pantothenate, 100 μg/ml streptomycin and 62.5 μg/ml penicillin. To induce differentiation, SGBS cells were washed repeatedly with PBS buffer and then cultured in serum-free medium supplemented with 10 nM insulin, 200 pM triiodothyronine, 1 μM cortisol, 2 μM BRL 49653, 0.115 mg/ml 1-methyl-3-isobutylxanthine (IBMX), 0.25 mmol/l dexamethasone (DEX), and 0.01 mg/ml human transferrin for 4 d. After 4 d, the medium was replaced with the differentiation medium lacking BRL 49653, IBMX, and DEX. These cells were used for the chromatin immunoprecipitation (ChIP) experiments on day 6 of differentiation.

Measuring ROS

For the DCF assay (Molecular Probes), primary human adipocytes were seeded in 96-well plates and differentiated for 6 d. On day 6, medium was changed to serum- and phenol red-free medium for 24 h. After 24 h, cells were preloaded with 5 μM DCF at 37°C for 1 h and then treated with various treatments for 3 h. Cells were then washed once with HBSS and fluorescence was immediately measured in a plate reader with an excitation/emission wavelength of 485–528 nm. DCF values were calculated after normalizing background fluorescence levels of DCF.

Measuring $[Ca^{2+}]_i$ levels

We determined $[Ca^{2+}]_i$ levels using Fluo-3 AM. Briefly, cells were preloaded with 5 μM Fluo-3 AM and an anionic detergent, 10% Pluronic F-127, at 37°C for 30 min in the dark. Cells were then washed with a buffer consisting of HBSS, CaCl$_2$, and probenecid, which prevents Fluo-3 AM leakage from cells. Baseline fluorescence was measured using a Synergy Multidetection Microplate Reader (BioTek Inc., Winooski, VT). Cells were then

treated with thapsigargin (positive control), CLA isomers, TMB-8, BAPTA, or EGTA and fluorescence was monitored at 10–20-s intervals for 8 min. Excitation wavelength was 485 nm, and fluorescence was collected at 528 nm. Changes in the ratio of calcium-dependent fluorescence to prestimulus background fluorescence (F/F_0) were plotted over time. For simplicity, single representative experiments are shown.

Immunoblotting

Immunoblotting was performed using 4%–12% NuPage pre-cast gels (Invitrogen) as previously described (7).

Chromatin immunoprecipitation (ChIP) assay

ChIP experiments were performed as previously described with minor modifications (8). Briefly, SGBS cells were grown and differentiated in 10-cm NUNC dishes and treated with BSA, CLA, or TMB-8. After treatment, cells were crosslinked, harvested in lysis buffer (i.e., 0.1% SDS, 1% Triton X-100, 150 mM NaCl, 1 mM EDTA, 20 mM Tris [pH 8.0], and 1× Complete proteinase inhibitor cocktail), and sonicated. DNA concentration was determined by measuring absorbance at 260 nm (A_{260}). Samples were diluted to equal concentrations and preincubated for 3 h with 2 µg NFκB p65 antibody (sc-372 Santa Cruz) and 40 µg BSA in a total volume of 400 µl lysis buffer. Protein A beads (20 µl) were washed three times in lysis buffer, diluted in lysis buffer to a total volume of 100 µl, and incubated for 2 h with 10 µg BSA. Following preincubation, prepared beads were added to the chromatin samples and incubated overnight. Beads were washed as previously described, and DNA was purified by phenol-chloroform extraction. Immunoprecipitated DNA and 5% input DNA were analyzed using real-time PCR.

Mitochondrial membrane integrity assays

Mitochondrial membrane potential and cytochrome C release were measured as indicators of potential mitochondrial stress caused by 10,12 CLA treatment. Chlorophenylhydrazone (CCCP) and antimycin A were used as positive controls for the membrane potential assay, and thapsigargin for cytochrome C release. The selective fluorescent probe JC-1 (Molecular Probes) was used to measure the membrane potential according to the manufacturer's instructions. Briefly, 5 µg/ml JC-1 was added to the cultures during the last 15 min of a 12-h treatment. Cultures were then washed with PBS, and the fluorescence (i.e., excitation 530 nm, emission 590 nm) was quantified in a Synergy Multidetection Microplate Reader. For determining the abundance of cytochrome C in the cytosol, cultures were harvested after 24 h of treatment and then subjected to subcellular fractionation to separate the cytosol from the mitochondria fraction as previously described (7). Subsequently, cytosolic cytochrome C levels were determined by immunoblotting.

RNA isolation and PCR

Total RNA was isolated from the cultures using Tri Reagent purchased from Molecular Research Center (Cincinnati, OH), according to manufacturer's protocol. For real-time PCR, 2.0 µg total RNA was converted into first strand cDNA using Applied Biosystems High-Capacity cDNA Archive Kit (Foster City, CA). Real-time PCR was performed in an Applied Biosystems 7500 FAST Real-Time PCR System using Taqman Gene Expression Assays. To account for possible variation in cDNA input or the presence of PCR inhibitors, the endogenous reference gene GAPDH was simultaneously quantified for each sample, and these data normalized accordingly. The Relative Standard Curve Method using seven, 2-fold dilutions ranging from 100 to 1.56 ng RNA was used to check primer efficiency and linearity of each transcript according to Applied Biosystem's "Guide to Performing Relative Quantification of Gene Expression Using Real-Time Quantitative PCR."

Measurement of PGF$_{2\alpha}$ levels

PGF$_{2\alpha}$ levels were measured according to a standard protocol provided by Cayman Chemicals for their PGF$_{2\alpha}$ enzyme immunoassay (EIA) kit. Medium was collected from cultures and assayed in duplicate at multiple dilutions.

[^{3}H]2-deoxy-glucose uptake

Newly differentiated cultures of human adipocytes were incubated in serum-free basal DMEM containing 1,000 mg/liter D-(+)-glucose with or without 20 pmol/l of human insulin. Cultures were treated with BSA vehicle, 50 µM 10,12 CLA, or 50 µM 10,12 CLA + 10 µM KN-62 for 48 h. Following treatment, insulin-stimulated uptake of [^{3}H]2-deoxy-glucose was measured following a 90-min incubation with 100 nmol/l human insulin as described previously (5).

Statistical analyses

One-way ANOVA was used to compare data unless otherwise indicated. Student's t-test was used to compute individual pairwise comparisons of least square means ($P < 0.05$). Data are expressed as mean ± SEM unless otherwise stated. All analyses were performed using JMP IN version 4.04 software (SAS Institute, Cary, NC).

RESULTS

10,12 CLA increases [Ca^{2+}]$_i$

To examine the effect of CLA isomers on [Ca^{2+}]$_i$ levels, we utilized the calcium-sensitive fluorescent dye Fluo-3 AM. Thapsigargin, a Ca^{2+}-ATPase inhibitor that depletes ER calcium stores (24), was used as a positive control. Thapsigargin increased intracellular calcium levels in a dose-dependent manner (**Fig. 1A**). Consistent with our hypothesis, 50–150 µM 10,12 CLA increased [Ca^{2+}]$_i$ in a dose-dependent manner (Fig. 1B). In contrast, 9,11 CLA modestly increased [Ca^{2+}]$_i$ levels compared to the vehicle control. Next, TMB-8 was used to determine the degree to which 10,12 CLA mobilized calcium specifically from the ER. As shown in Fig. 1C, TMB-8 attenuated the immediate increase in [Ca^{2+}]$_i$ mediated by thapsigargin and 10,12 CLA, suggesting that 10,12 CLA also stimulates calcium release from the ER. Whereas preincubation of Fluo-3–loaded adipocytes with the [Ca^{2+}]$_i$ chelator BAPTA completely blocked thapsigargin-mediated increase in [Ca^{2+}]$_i$ (Fig. 1D), BAPTA attenuated the immediate, but not the sustained, effects of 10,12 CLA on [Ca^{2+}]$_i$ (Fig. 1D). In contrast, EGTA attenuated the sustained, but not the immediate 10,12 CLA–mediated increase of [Ca^{2+}]$_{i,}$ suggesting that extracellular calcium may play a role in the sustained regulation of [Ca^{2+}]$_i$ by 10,12 CLA (Fig. 1E). Lastly, to determine the extent to which CLA causes calcium release only from the ER, cultures were pretreated with thapsigargin followed by a second treatment with thapsigargin or 10,12 CLA, and vice-versa. As expected, thapsigargin pretreatment completely blocked thapsigargin from increasing [Ca^{2+}]$_i$, demonstrating that thapsigargin depletes ER calcium in human adipocytes (Fig. 1F). Furthermore, thapsigargin pretreatment attenuated 10,12
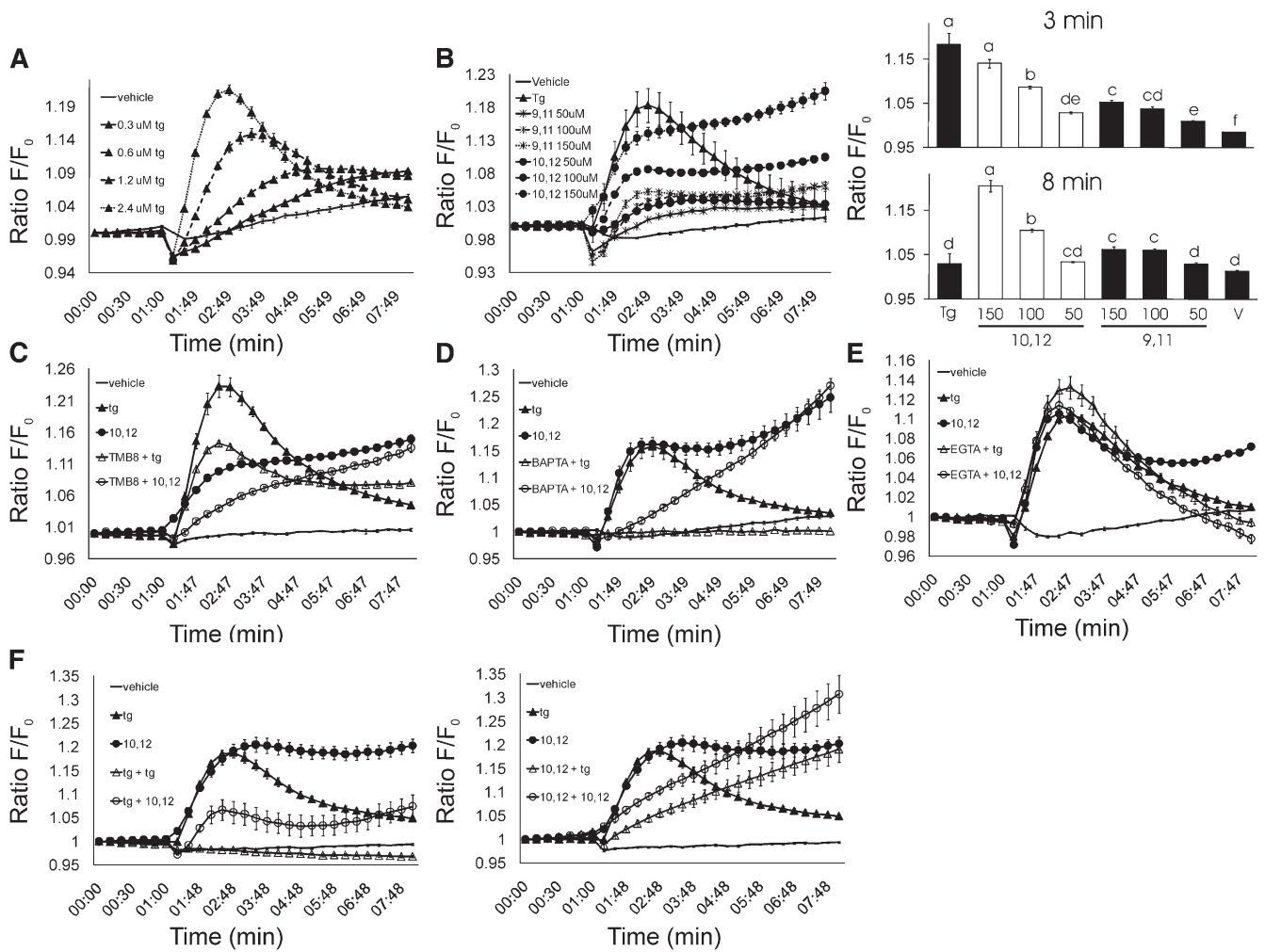
Fig. 1. 10,12 CLA increases $[Ca^{2+}]_i$ in an isomer-specific and dose-dependent manner. Cultures of newly differentiated human adipocytes were preloaded with 5 µM Fluo-3 AM. A: Cultures were injected with vehicle (−), or 0.3, 0.6, 1.2, or 2.4 µM thapsigargin (Tg; triangle up filled), a positive control that causes the release of calcium from the ER. B: Cultures were injected with vehicle (−); 5 µM Tg (triangle up filled); 50, 100, or 150 µM 10,12 CLA (circle filled); or 50, 100, or 150 µM 9,11 CLA (star filled). The line graph on the left shows the time course for $[Ca^{2+}]_i$, and bar graphs on the right show the peak $[Ca^{2+}]_i$ levels at the 3 and 8 min treatment times. C: Cultures were injected with vehicle (−), Tg (triangle up filled); 150 µM 10,12 CLA (circle filled); 100 µM TMB-8 (blocks ER calcium release) + 5 µM Tg (triangle up open); or 100 µM TMB-8 + 150 µM 10,12 CLA (circle open). D: Cultures were injected with vehicle (−); 5 µM Tg (triangle up filled); 150 µM 10,12 CLA (circle filled); 10 µM BAPTA (an intracellular calcium chelator) + Tg (triangle up open); or 10 µM BAPTA+ 150 µM 10,12 CLA (circle open). E: Cultures were injected with vehicle (−); 5 µM Tg (triangle up filled), 150 µM 10,12 CLA (circle filled), 100 µM EGTA (extracellular calcium chelator) + Tg (triangle up open), or 100 µM EGTA + 150 µM 10,12 CLA (circle open). F: Cultures were injected with vehicle (−), 5 µM Tg (triangle up filled), or 150 µM 10,12 CLA (circle filled), or pretreated for 7 min with 5 µM Tg followed by a second treatment with 5 µM Tg (triangle up open) or 150 µM 10,12 CLA (circle open) (left side) and vice-versa (right side) to determine the extent to which CLA causes calcium release specifically from the ER. Emitted fluorescence intensities were collected over time using a multidetection microplate reader. Excitation wavelength was 485 nm, and fluorescence was collected at 528 nm. Means (± SEM; n = 4–6) in all panels are representative of at least three independent experiments.
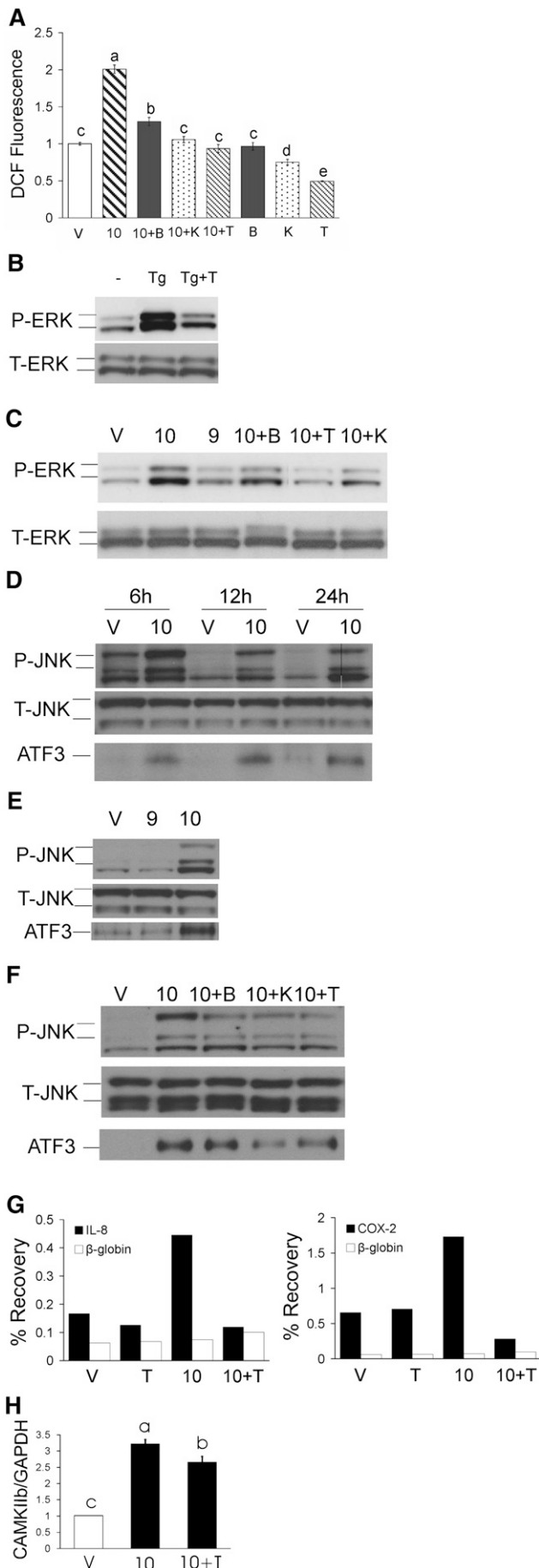
CLA from increasing $[Ca^{2+}]_i$ levels. In contrast, 10,12 CLA pretreatment only attenuated the immediate effects of 10,12 CLA and thapsigargin on $[Ca^{2+}]_i$. In fact, CLA pretreatment augmented the sustained increase in $[Ca^{2+}]_i$ levels by 10,12 CLA, even in cells treated with thapsigargin (Fig. 1F). Collectively, these data suggest that 10,12 CLA increases $[Ca^{2+}]_i$ initially, but not exclusively, from the ER.

10,12 CLA production of ROS and activation of ERK1/2, JNK, and NFκB are dependent on $[Ca^{2+}]_i$ and CaMKII

To determine the extent to which CLA-mediated production of ROS and activation of MAPK and NFκB were

dependent on $[Ca^{2+}]_i$, we investigated the effects of calcium chelators and inhibitors on ROS, ERK1/2, JNK, ATF3, and NFκB in CLA-treated cultures. ROS production was increased by 50 µM 10,12 CLA within 3 h in an isomer-specific manner (**Fig. 2A**; 9,11 CLA data not shown), which was blocked by BAPTA, TMB-8, and KN-62, a CaMKII inhibitor.

Phosphorylation of ERK1/2 by thapsigargin was attenuated by TMB-8 (Fig. 2B), confirming that calcium release from the ER increases ERK1/2 activation. Similarly, 10,12 CLA increased the phosphorylation of ERK1/2 within 12 h in an isomer-specific manner (Fig. 2C), which was attenu-

A
DCF Fluorescence
V 10 10+B 10+K 10+T B K T

B
- Tg Tg+T
P-ERK
T-ERK

C
V 10 9 10+B 10+T 10+K
P-ERK
T-ERK

D
6h 12h 24h
V 10 V 10 V 10
P-JNK
T-JNK
ATF3

E
V 9 10
P-JNK
T-JNK
ATF3

F
V 10 10+B 10+K 10+T
P-JNK
T-JNK
ATF3

G
% Recovery — IL-8, β-globin
V T 10 10+T
% Recovery — COX-2, β-globin
V T 10 10+T

H
CAMKIIb/GAPDH
V 10 10+T

ated by BAPTA, TMB-8, and KN-62 (Fig. 2C). Consistent with these data, 10,12 CLA activation of JNK (Fig. 2D–F) was also attenuated by BAPTA, TMB-8, and KN-62 (Fig. 2F), while KN-62 and TMB-8 attenuated 10,12 CLA's increase of ATF3 protein levels. These data suggest that ROS, ERK1/2, JNK, and ATF3 are downstream targets of 10,12 CLA–mediated $[Ca^{2+}]_i$ signaling and calcium-dependent CaMKII.

To investigate the role of calcium in mediating 10,12 CLA activation of NFκB, cultures of human SGBS adipocytes were pretreated with 100 μM TMB-8 for 1 h and then treated over time (3–12 h) with 30 μM 10,12 CLA. SGBS cells were used because of the large number of cells needed to the perform ChIP assay. NFκB binding to inflammatory genes was subsequently analyzed using ChIP. Ten hour treatment with 10,12 CLA increased NFκB binding to the IL-8 and COX-2 promoters, which was blocked by TMB-8 (Fig. 2G). These data suggest that 10,12 CLA induction of NFκB binding to inflammatory genes is mediated, in part, by calcium release from the ER.

Based on KN-62 attenuating CLA induction of ROS and MAPK activation, the impact of 10,12 CLA on CaMKII

Fig. 2. 10,12 CLA increase of ROS, ERK, JNK, ATF3, and NFκB are attenuated by BAPTA, TMB-8, or KN-62. Cultures of newly differentiated human adipocytes were serum-starved 24 h and then treated with CLA, the calcium chelators, or inhibitors. A: Cultures were preloaded with DCF for 1 h, pretreated for 1 h with 2 μM BAPTA (B), 10 μM KN-62 (K), or 100 μM TMB-8 (T), and then treated with BSA vehicle (V) or 50 μM 10,12 CLA (10) for 3 h. Emitted fluorescence intensities were measured using a multidetection microplate reader. Excitation wavelength was 485 nm and fluorescence was collected at 528 nm. One-way ANOVA was used to compare data. Means (± SEM; n = 12) that do not share a common lower case letter differ (P < 0.05). B: Cultures were treated for 12 h with 30 nM thapsigargin (Tg) in the absence or presence of TMB-8 (T). C: Cultures were treated for 12 h with BSA vehicle (V), 50 μM 10,12 CLA alone (10), 50 μM 9,11 CLA alone (9), or 50 μM 10,12 CLA in the presence of 2 μM BAPTA (10+B), 10 μM KN-62 (10+K), or 100 μM TMB-8 (10+T). Proteins were then harvested, subjected to electrophoresis, and immunoblotted for p-ERK and total ERK. D: Cultures were treated with BSA vehicle (V) or 50 μM 10,12 CLA (10) for 6, 12, or 24 h and then immunoblotted for p-JNK, total JNK and ATF3. E, Cultures were treated for 12 h with BSA vehicle (V) 50 μM 9,11CLA (9), or 50 μM 10,12 CLA (10) and immunoblotted as in D. F: Cultures were treated for 12 h with BSA vehicle (V) or 50 μM 10,12 CLA (10) alone or 10,12 CLA in the presence of 2 μM BAPTA (10+B), 10 μM KN-62 (10+K), or 100 μM TMB-8 (10+T) and immunoblotted as in D. G: Cultures of newly differentiated SGBS cells were treated for approximately 10 h with BSA vehicle (V), 30 μM 10,12 CLA (10) in the absence or presence of 100 μM TMB-8 (T). ChIP assays quantified DNA-binding of NFκB to the IL-8 and COX-2 proximal promoters using real-time PCR with primers positioned at NFκB response elements (black bars). Primers positioned at the β-globin promoter (white bars) were used as "no binding" control. Results are shown as percent recovery relative to input. H: Cultures of newly differentiated human adipocytes were serum-starved for 24 h and then treated for 12 h with BSA vehicle (V) or 50 μM 10,12 CLA (10), or 50 μM 10,12 CLA + 100 μM TMB-8 (10+T) and then harvested for real-time PCR analysis of CaMKII mRNA levels. One-way ANOVA was used to compare data. Means (± SEM; n = 5) that do not share a common lower case letter differ (P < 0.05). Data in all panels are representative of at least two independent experiments.

mRNA levels was examined. We found that 10,12 CLA treatment for 12 h induced CaMKII β mRNA by approximately 200% (Fig. 2H), which was modestly attenuated by TMB-8. However, 10,12 CLA did not increase the mRNA levels of the more abundant isoforms of CaMKII (i.e., α, γ, and δ; data not shown).

10,12 CLA–mediated increase of $[Ca^{2+}]_i$ is linked to inflammatory gene expression but not to mitochondrial stress

The integrated stress response (ISR) has been recently shown to play a role in 10,12 CLA induction of inflammation (25). To determine the effect of CLA on ISR and inflammatory gene expression, cultures were treated with 9,11 CLA or 10,12 CLA for 6, 12, 24, or 48 h. Our results show that 30 μM and 100 μM 10,12 CLA (data not shown) increased the expression of ISR genes (i.e., ATF3, CHOP, GADD34) within 6–12 h (**Fig. 3A**), and inflammatory genes (i.e., IL-6, IL-8, IL-1β, COX-2) by 12 h (Fig. 3A) in an isomer-specific manner. Because metabolic stress can cause calcium release from mitochondria, we analyzed two indicators of mitochondrial membrane integrity, mitochondrial JC-1 staining and cytochrome C release. However, neither JC-1 staining nor cytosolic cytochrome C abundance were affected by 10,12 CLA (Fig. 3B), suggesting that 10,12 CLA does not adversely affect mitochondrial membrane potential or integrity.

Next, we determined the ability of calcium release from the ER to induce inflammation. Thapsigargin induced IL-8 and IL-6 gene expression, which was attenuated by TMB-8 (**Fig. 4A**). Subsequently, we investigated the role of $[Ca^{2+}]_i$ in mediating CLA induction of ISR and inflammatory genes by pretreating cultures with BAPTA or TMB-8, and then treating with 30 μM 10,12 CLA for 12 h. BAPTA completely blocked 10,12 CLA induction of IL-8, IL-6, CHOP, and GADD34 (Fig. 4B). In addition, BAPTA reduced COX-2 gene expression by 70%, while decreasing ATF3 gene expression by 44% (Fig. 4B). Treatment with TMB-8 suppressed the 10,12 CLA-induced expression of IL-8, IL-6, COX-2, CHOP, and GADD34 (Fig. 4B), while only modestly reducing ATF3 mRNA levels. To determine the role of CaMKII in mediating 10,12 CLA induction of ISR and inflammatory genes, cultures were pretreated with KN-62. KN-62 attenuated or blocked induction of IL-8, IL-6, COX-2, CHOP, GADD34, and ATF3 gene expression (Fig. 4B). These data suggest that 10,12 CLA induction of ISR and inflammatory genes is linked to CaMKII activation and calcium release from the ER. However, direct analysis of CaMKII activity is needed to verify this suggestion.

Phospholipase C activity plays a role in 10,12 CLA–mediated inflammation

We investigated the role of phospholipase C (PLC), a membrane-bound, signal transduction protein involved in the release of calcium from intracellular stores (26), using the PLC inhibitor D609. D609 attenuated 10,12 CLA increase of $[Ca^{2+}]_i$ (**Fig. 5A**), ROS (Fig. 5B), and ISR and inflammatory gene expression (Fig. 5C). These data suggest that PLC activity plays a role in 10,12 CLA mobilization of calcium, increase of ROS, and ISR and inflammatory gene expression.

10,12 CLA activates the inflammatory PG pathway independently of $[Ca^{2+}]_i$

$PGF_{2\alpha}$ has been shown to suppress adipogenesis (23) and is associated with inflammation and insulin resistance in humans consuming CLA supplements (10–12). Consistent with these findings, 10,12 CLA increased COX-2 gene expression (Fig. 4B), which was decreased by BAPTA, TMB-8, and KN-62. For these reasons, we investigated the role of $[Ca^{2+}]_i$ in 10,12 CLA induction of the inflammatory PG pathway. Activation of PLA_2 occurred within 12 h of 10,12 CLA treatment (**Fig. 6A**) and was isomer-specific (Fig. 6B). However, neither BAPTA nor TMB-8 suppressed 10,12 CLA–mediated phosphorylation of PLA_2 (Fig. 6C) nor increased levels of $PGF_{2\alpha}$ after 24 h of treatment (Fig. 6D), while KN-62 had only a modest effect. Collectively, these data show that chronic 10,12 CLA treatment robustly increases inflammatory $PGF_{2\alpha}$ production in human adipocytes in vitro as it does in humans in vivo and that this effect appears to be relatively independent of $[Ca^{2+}]_i$ levels or CaMKII activity.

10,12 CLA–mediated insulin resistance is prevented by KN-62

KN-62 blocked 10,12 CLA suppression of PPARγ protein levels after 48 h of treatment (**Fig. 7A**), while TMB-8 had no effect. Similarly, KN-62 blocked 10,12 CLA induction of SOCS-3 gene expression (Fig. 7B) and attenuation of insulin-stimulated glucose uptake after 48 h of treatment (Fig. 7C), but TMB-8 had no effect (data not shown). These data demonstrate that chronic treatment with 10,12 CLA causes insulin resistance in human adipocytes that appears to depend on CaMKII activation but not directly on calcium release from the ER.

DISCUSSION

The purpose of this study was to determine the role of $[Ca^{2+}]_i$ in mediating 10,12 CLA–induced ROS production, inflammatory mRNA and protein levels, and insulin resistance in human adipocytes. Collectively these data provide support for our working model shown in **Fig. 8**, suggesting that 10,12 CLA's impact on calcium signaling and markers of inflammation and insulin resistance occurs in two response phases. The initial response to CLA begins with an immediate and sustained release of calcium from the ER, and possibly other sources like the extracellular compartment, which leads to ROS production, MAPK and NFκB activation, and ISR and inflammatory gene expression. The second and more chronic response begins with PLA_2 activation and $PGF_{2\alpha}$ production, which appears to be independent of calcium. This causes another phase of calcium signaling that further activates CaMKII, leading to the suppression of PPARγ and the development of insulin resistance. Consistent with this second phase of calcium signaling involving CaMKII, $PGF_{2\alpha}$
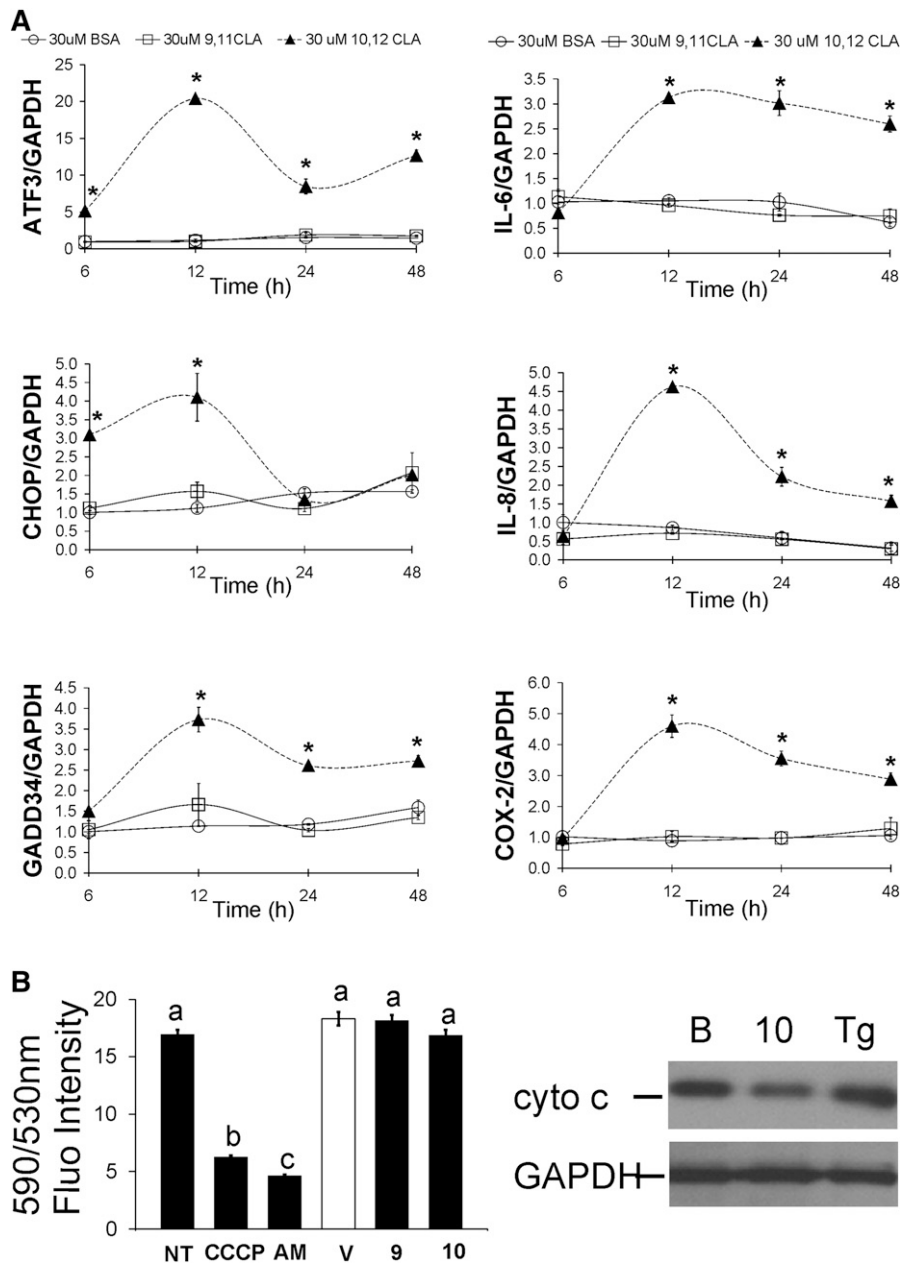
Fig. 3. Time course of CLA–mediated increase in stress-related and inflammatory gene expression. A: Cultures of newly differentiated human adipocytes were serum-starved for 24 h and then treated for 6, 12, 24, or 48 h with BSA vehicle (circle open), 30 μM *cis*-9, *trans*-11 CLA (square open), or 30 μM *trans*-10, *cis*-12 CLA (triangle up filled), and then harvested. RNA was isolated and the mRNA levels of ATF3, CHOP, GADD34, IL-6, IL-8, COX-2, and GAPDH (load control) were measured using real-time PCR. Means (± SEM; n = 2) with asterisks (*) differ significantly ($P < 0.05$) from the BSA controls at each time point, and are representative of at least two independent experiments. Statistical analyses were performed for data testing the main effects of treatment (BSA, 10,12 CLA, 9,11 CLA) and time (6, 12, 24, 48 h) and their interaction. B: To measure indicators of mitochondrial stress (i.e., less JC-1 staining and more cytoplasmic cytochrome C), cultures of human adipocytes were treated vehicle control (NT), the positive controls CCCP (20 μM), antimycin A (AM, 20 nM), or thapsigargin (Tg), or BSA vehicle (V), 50 μM 9,11 CLA (9), or 50 μM 10,12 CLA (10) for 12 h (JC-1 staining) or 24 h (cytochrome C [cyto C] release). For the JC-1 assay, fluorescence was measured at 590 and 530 nm. Means (± SE; n = 6–12) that do not share a common lowercase letter differ ($P < 0.05$). Data are representative of two independent experiments. One-way ANOVA was used to compare data. For the cytochrome C release assay, cells were harvested and subcellular fractionation was performed to collect mitochondrial and cytosolic proteins. The cytosolic fraction was immunoblotted for cytochrome C and GAPDH. Data are representative of one independent experiment.
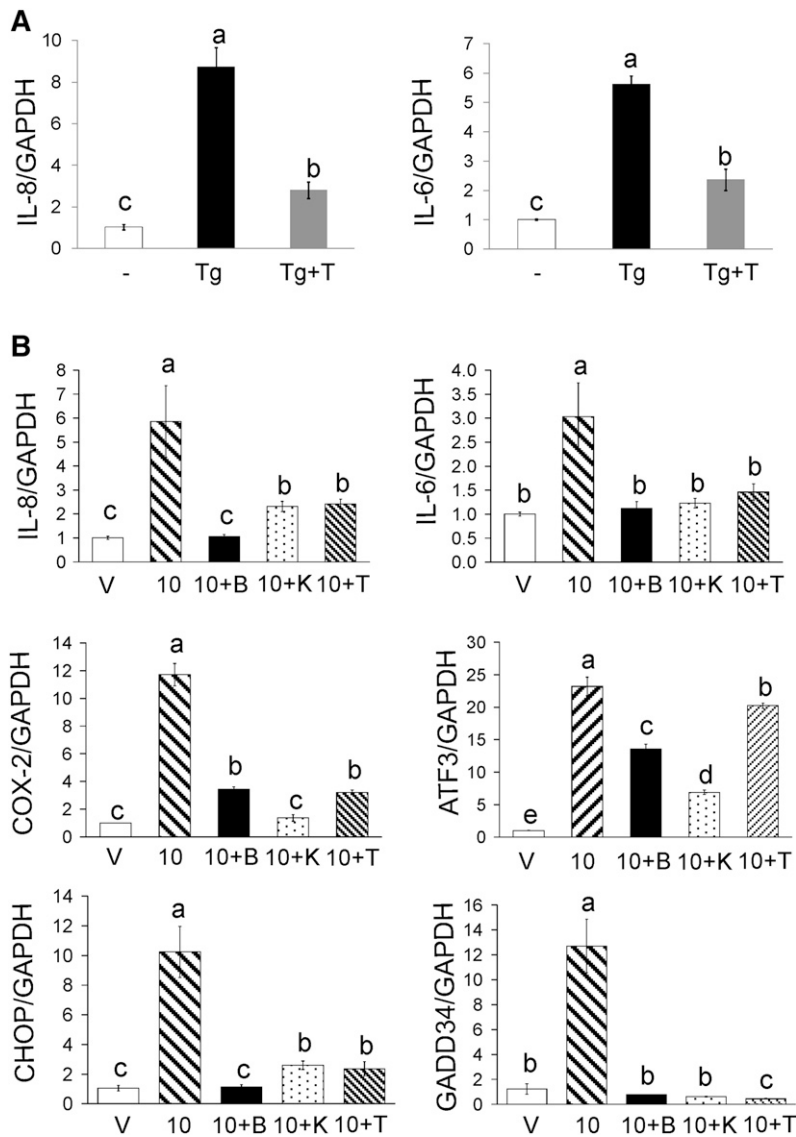
Fig. 4. 10,12 CLA-induced inflammatory and ISR gene expression are dependent on $[Ca^{+2}]_i$. A: Cultures of newly differentiated human adipocytes were treated for 12 h with thapsigargin (Tg) in the absence or presence of 100 µM TMB-8 (T). B: Cultures were treated for 12 h with BSA vehicle (V), 50 µM 10,12 CLA alone (10), or 10,12 CLA in the presence of 2 µM BAPTA (10+B), 10 µM KN-62 (10+K), or 100 µM TMB-8 (10+T). A and B: RNA was subsequently isolated and the mRNA levels of IL-8, IL-6, COX-2, ATF-3, CHOP, GADD34, or GAPDH were measured by real-time PCR. Data are normalized to the vehicle controls. Means (± SEM; n = 2) that do not share a common lower case letter differ ($P < 0.05$). Data are representative of three independent experiments. One-way ANOVA was used to compare data.

has been reported to increase $[Ca^{2+}]_i$ levels and activate CaMKII in murine adipocytes, leading to decreased adipocyte differentiation (23).

In support of our findings, calcium and ROS have been implicated in the activation of NFκB and inflammation (27). Likewise, we found that blocking calcium signaling with BAPTA, TMB, or KN-62 prevented CLA–mediated ROS production (Fig. 2A), suggesting that increased $[Ca^{2+}]_i$ levels precede ROS production in human adipocytes. Furthermore, these compounds attenuated 10,12 CLA–mediated activation of MAPKs (Fig. 2B–F) and NFκB (Fig. 2G), and the expression of ISR and inflammatory genes (Fig. 4). Consistent with these data, the PLC inhibitor D609 attenuated 10,12 CLA increase in $[Ca^{2+}]_i$ levels, ROS, and inflammatory gene expression (Fig. 5). Collectively, these data demonstrate the important role of $[Ca^{2+}]_i$ in mediating ROS and inflammatory responses to 10,12 CLA in cultures of human adipocytes.

The prevention of CLA–mediated insulin resistance by KN-62, but not TMB-8, suggests that 10,12 CLA increased

$[Ca^{2+}]_i$ levels from sources other than the ER. Although KN-62 was initially identified as a calcium-CaMKII inhibitor, this inhibitor has also been reported to block voltage-sensitive channels (28–31). Thus, it seemed possible that 10,12 CLA increases Ca^{2+} influx across the plasma membrane. Although, KN-62 (data not shown) and the extracellular calcium chelator EGTA did not dramatically affect 10,12 CLA's immediate increase of $[Ca^{2+}]_i$ (Fig. 1E), EGTA attenuated the sustained effects of 10,12 CLA on $[Ca^{2+}]_i$, suggesting that extracellular calcium influx may be an important for sustaining $[Ca^{2+}]_i$, at least for the short term. In agreement with other studies, the phosphatidylcholine-specific (PC)-PLC inhibitor D609 (Fig. 5A) attenuated 10,12 CLA's immediate increase in $[Ca^{2+}]_i$ levels. Activation of PC-PLC has been reported to increase $[Ca^{2+}]_i$ levels via conversion of diacylglycerol (DAG) by DAG kinase to phosphatidic acid, which mobilizes calcium from inositiol-3-phosphate–independent calcium pools (26, 31–33). Therefore, it appears that 10,12 CLA initially stimulates an efflux of calcium from intracellular stores like the ER, followed by calcium
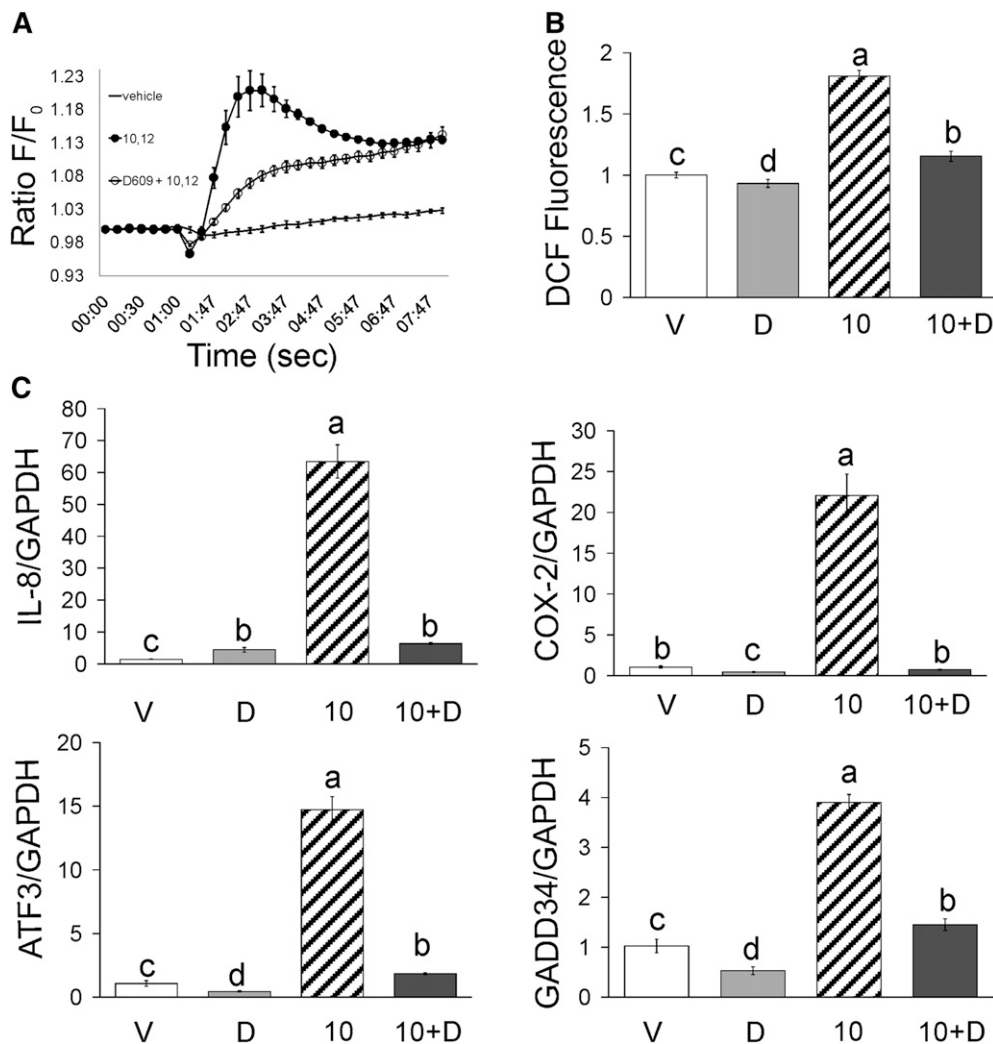
Fig. 5. 10,12 CLA increase of $[Ca^{2+}]_i$, ROS levels and expression of inflammatory and ISR genes are dependent on PLC. A: Cultures of newly differentiated human adipocytes were preloaded with 5 μM Fluo-3 AM. Cultures were injected with vehicle (−), 50 μM 10,12 CLA (circle filled), or 25 μM D609 pretreatment + 50 μM 10,12 CLA (circle open). Emitted fluorescence intensities were collected over time using a multidetection microplate reader. Excitation wavelength was 485 nm, and fluorescence was collected at 528 nm. Means (± SEM; n = 4) are representative of two independent experiments. B: Cultures of newly differentiated human adipocytes were preloaded with DCF for 30 min. Cultures were then treated with BSA vehicle (V) or 50 μM 10,12 CLA (10) alone for 12 h, or pretreated for 30 min with 50 μM D609 followed by 12-h treatment with BSA vehicle (D) or 50 μM 10,12 CLA (10+D). Emitted fluorescence intensities were measured using a multidetection microplate reader. Excitation wavelength was 485 nm, and fluorescence was collected at 528 nm. Means (± SEM; n = 3–12) are representative of three independent experiments. C: Cultures were pretreated for 30 min with 50 μM D609 (D) followed by 12-h treatment with BSA vehicle (V) or 50 μM 10,12 CLA (10). RNA was subsequently isolated and mRNA levels of IL-8, COX-2, ATF-3, GADD34, and GAPDH were measured by real-time PCR. Data are normalized to the vehicle controls. Means (± SEM; n = 2) that do not share a common lower case letter differ ($P < 0.05$). Data are representative of three independent experiments. One-way ANOVA was used to compare data.

influx from extracellular sources, possibly to replenish ER calcium.

The mitochondria can also store and release calcium, potentially providing another source of $[Ca^{2+}]_i$ for signaling (34). Mitochondrial dysfunction or stress, similar to ER stress, can adversely affect the mitochondria's capacity for calcium storage or regulated release, thereby increasing $[Ca^{2+}]_i$ levels. For example, treating cells with a mitochondrial uncoupler increases $[Ca^{2+}]_i$ levels, thereby activating ERK1/2 (35). Similarly, impairing mitochondrial respiration increases $[Ca^{2+}]_i$ levels and activates CaMKIV (36). To this end, we investigated whether 10,12 CLA could affect mitochondria function by examining two indicators of altered mitochondrial membrane potential or integrity (i.e., the JC-1 assay and cytochrome C release from mitochondria, respectively). Neither marker of mitochondrial dysfunction was affected by 10,12 CLA (Fig. 3B), suggesting that acute 10,12 CLA treatment does not directly cause mitochondrial dysfunction.
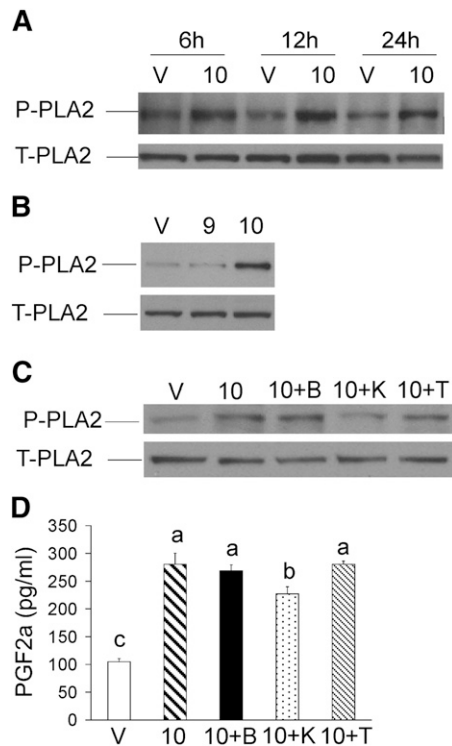
Fig. 6. 10,12 CLA activation of the inflammatory PG pathway is not dependent on $[Ca^{2+}]_i$. A: Cultures of newly differentiated human adipocytes were treated with BSA vehicle (V) or 30 μM 10,12 CLA (10) for 6, 12, or 24 h. Cells were harvested and immunoblotted for p-PLA2 and total PLA2. B: Cultures were treated for 12 h with BSA vehicle (V), 30 μM 9,11 CLA (9), or 30 μM 10,12 CLA (10), and immunoblotted as in A. Data are representative of three experiments. C: Cultures were treated for 12 h with BSA vehicle (V), 50 μM 10,12 CLA alone (10), or 10,12 CLA in presence of 2 μM BAPTA (10+B), 10 μM KN-62 (10+K), or 100 μM TMB-8 (10+T), and immunoblotted as in A. D: Cultures were treated for 24 h with BSA vehicle (V), 50 μM 10,12 CLA alone (10), or 10,12 CLA in the presence of 2 μM BAPTA (10+B), 10 μM KN-62 (10+K), or 100 μM TMB-8 (10+T). Conditioned media were subsequently collected and $PGF_{2\alpha}$ levels were measured using a commercially available EIA kit. Means (± SEM; n = 2) not sharing a common lower case letter differ ($P < 0.05$). Data in all panels are representative of three independent experiments. One-way ANOVA was used to compare data.

Fig. 7. 10,12 CLA–mediated insulin resistance is attenuated by KN-62. A: Cultures of newly differentiated human adipocytes were treated for 48 h with BSA vehicle (V); 50 μM 10,12 CLA (10); 10,12 CLA + 10 μM KN-62 (10+K); 10,12 CLA + 100 μM TMB (10+T); 10 μM KN-62 (K); or 100 μM TMB-8 (T). Cultures were harvested and immunoblotted for PPARγ and GAPDH. B: Cultures were treated for 48 h with BSA vehicle (V); 50 μM 10,12 CLA alone (10); or 10,12 CLA in the presence of 10 μM KN-62 (10+K). Cells were harvested for RNA, and SOCS-3 and GAPDH were measured by real-time PCR. C: Cultures were treated for 48 h with BSA vehicle (V); 50 μM 10,12 CLA alone (10); or 10,12 CLA in the presence of 10 μM KN-62 (10+K). Uptake of basal or insulin-stimulated [³H]2-deoxy-glucose was subsequently measured in cultures treated without (−) or with (+) insulin. Means (± SEM; n = 3) that do not share a common lower case letter differ ($P < 0.05$). Data in all panels are representative of three independent experiments. One-way ANOVA was used to compare data.

G protein-coupled receptor (GPCR) agonists, depolarizing stimuli, or ionophores have been reported to increase free $[Ca^{2+}]_i$ levels, thereby activating CaMKII and its downstream targets such as ERK1/2 (37–41). Similarly, we previously demonstrated that the GPCR antagonist pertussis toxin blocked 10,12 CLA–mediated activation of ERK1/2 (4). In the present study, we demonstrated the KN-62 also attenuates 10,12 CLA phosphorylation of ERK1/2 and JNK (Fig. 2C, F). KN-93, another CaMK inhibitor, has also been shown to attenuate lipopolysaccharide activation of ERK1/2, JNK, NFκB, and AP-1, a target of JNK (42). Collectively, these data support our hypothesis that CLA's activation of ERK1/2 and JNK are closely linked to $[Ca^{2+}]_i$ and CaMK activity.

We provide data demonstrating that the CaMKII inhibitor KN-62 prevents 10,12 CLA–mediated insulin resistance (Fig. 7). Elevate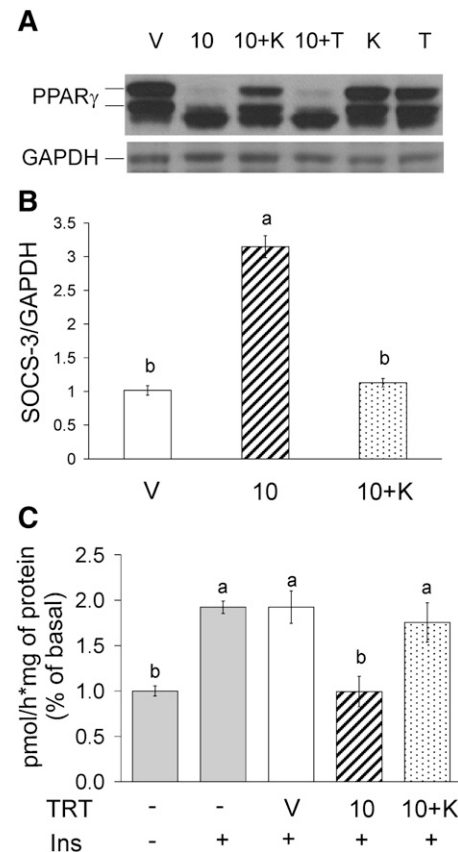d $[Ca^{2+}]_i$ levels have been linked to insulin resistance in insulin-sensitive cells (43–45), including rat adipocytes (46). In vivo, BAPTA was shown to reverse insulin resistance in rats fed a high-fat diet (47). Unfortunately, we could not use BAPTA for our glucose uptake studies due to its toxicity when used chronically (48 h). Furthermore, we were unable to consistently demonstrate that CLA increased phosphorylation or total CaMKII protein levels (data not shown). Therefore, although 10,12 CLA increased CaMKII β mRNA by 200%, we could not determine whether it increases CaMKII β protein abundance or activity. Future studies directly measuring CaMKII β activity and employing gene silencing techniques are needed to define the specific role of CaMKIIβ signaling on inflammation and insulin sensitivity in CLA-treated cultures of human adipocytes.
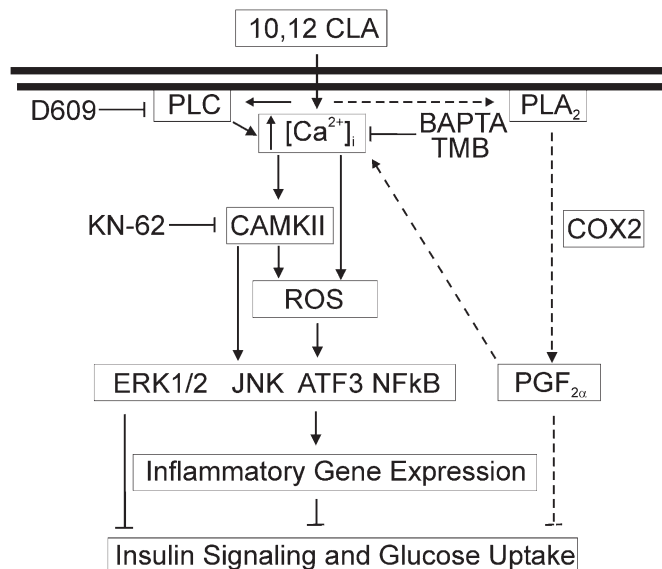
Fig. 8. Working model: 10,12 CLA–mediated oxidative stress, inflammation, and insulin resistance are regulated, in part, by $[Ca^{2+}]_i$. Acutely, 10,12 CLA increases $[Ca^{2+}]_i$ levels, which are dependent on PLC activity and mobilization of calcium from the ER initially, which is sustained by an influx of calcium from extracellular sources. This increase activates ROS and CaMKII, which in turn activate MAPK and NFκB that trigger ISR and inflammatory gene expression. The second and more chronic response to 10,12 CLA begins with PLA_2 activation and $PGF_{2\alpha}$ production, which appears to be independent of calcium. This causes another phase of calcium signaling that further activates CaMKII, leading to the suppression of PPARγ and the development of insulin resistance.

Delipidation of murine adipocytes by 10,12 CLA in vivo and in vitro has recently been linked to the ISR pathway (25). These authors demonstrated that 10,12 CLA, but not 9,11 CLA, induced markers of the ISR pathway in mouse and 3T3-L1 adipocytes. They also suggest that the ISR precedes the later induction of inflammatory gene expression and contributes to delipidation by 10,12 CLA. Our data in cultures of human adipocytes are similar to these published data in murine adipocytes. In addition, 10,12 CLA has been shown to cause atypical ER stress in a murine mammary carcinogenesis model (48). Similarly, the rapid (1 min) and chronic increase in $[Ca^{2+}]_i$ levels by 10,12 CLA appears to increase ROS production (3 h) and activate specific MAPKs (6 h) and ISR stress response genes (6–12 h) relatively early, which in turn, may lead to chronic (48 h) activation of CaMKII and subsequent insulin resistance in cultures of human adipocytes. However, the specific mechanism by which 10,12 CLA increases $[Ca^{2+}]_i$, and its direct effect on CaMKII activity require further investigation.

REFERENCES

1. Centers for Disease Control and Prevention. US Obesity Trends, 1985–2006. Accessed 2007 at http://www.cdc.gov/nccdphp/dnpa/obesity/trend/maps/index.htm.
2. Kennedy, A., K. Martinez, S. Schmidt, S. Mandrup, K. Lapoint, and M. McIntosh. 2009. Anti-obesity mechanisms of action of conjugated linoleic acid. *J. Nutr. Biochem.* **21:** 171–179.
3. Whigham, L. D., A. C. Watras, and D. A. Schoeller. 2007. Efficacy of conjugated linoleic acid for reducing fat mass: a meta-analysis in humans. *Am. J. Clin. Nutr.* **85:** 1203–1211.
4. Granlund, L., L. K. Juvet, J. I. Pedersen, and H. I. Nebb. 2003. Trans10, cis12-conjugated linoleic acid prevents triacylglycerol accumulation in adipocytes by acting as a PPARgamma modulator. *J. Lipid Res.* **44:** 1441–1452.
5. Brown, J. M., M. S. Boysen, S. Chung, O. Fabiyi, R. F. Morrison, S. Mandrup, and M. K. McIntosh. 2004. Conjugated linoleic acid induces human adipocyte delipidation: autocrine/paracrine regulation of MEK/ERK signaling by adipocytokines. *J. Biol. Chem.* **279:** 26735–26747.
6. Brown, J. M., M. S. Boysen, S. S. Jensen, R. F. Morrison, J. Storkson, R. Lea-Currie, M. Pariza, S. Mandrup, and M. K. McIntosh. 2003. Isomer-specific regulation of metabolism and PPARgamma signaling by CLA in human preadipocytes. *J. Lipid Res.* **44:** 1287–1300.
7. Chung, S., J. M. Brown, J. N. Provo, R. Hopkins, and M. K. McIntosh. 2005. Conjugated linoleic acid promotes human adipocyte insulin resistance through NFkappaB-dependent cytokine production. *J. Biol. Chem.* **280:** 38445–38456.
8. Nielsen, R., L. Grontved, H. G. Stunnenberg, and S. Mandrup. 2006. Peroxisome proliferator-activated receptor subtype- and cell-type-specific activation of genomic target genes upon adenoviral transgene delivery. *Mol. Cell. Biol.* **26:** 5698–5714.
9. Chung, S., J. M. Brown, M. B. Sandberg, and M. McIntosh. 2005. Trans-10,cis-12 CLA increases adipocyte lipolysis and alters lipid droplet-associated proteins: role of mTOR and ERK signaling. *J. Lipid Res.* **46:** 885–895.
10. Basu, S., U. Riserus, A. Turpeinen, and B. Vessby. 2000. Conjugated linoleic acid induces lipid peroxidation in men with abdominal obesity. *Clin. Sci.* **99:** 511–516.
11. Riserus, U., S. Basu, S. Jovinge, G. N. Fredrikson, J. Arnlov, and B. Vessby. 2002. Supplementation with conjugated linoleic acid causes isomer-dependent oxidative stress and elevated C-reactive protein: a potential link to fatty acid-induced insulin resistance. *Circulation.* **106:** 1925–1929.
12. Riserus, U., P. Arner, K. Brismar, and B. Vessby. 2002. Treatment with dietary trans10cis12 conjugated linoleic acid causes isomer-specific insulin resistance in obese men with the metabolic syndrome. *Diabetes Care.* **25:** 1516–1521.
13. Tholstrup, T., M. Raff, E. Straarup, P. Lund, J. Bruun, and S. Basur. 2007. Opposing effects of trans-10, cis-12 conjugated linoleic acid and cis-9, trans-11 conjugated linoleic acid on risk markers for coronary heart disease. *FASEB J.* **21:** A728.
14. Zemel, M. B. 1998. Nutritional and endocrine modulation of intracellular calcium: implications in obesity, insulin resistance and hypertension. *Mol. Cell. Biochem.* **188:** 129–136.
15. Martin, L., S. C. Pingle, D. M. Hallam, L. P. Rybak, and V. Ramkumar. 2006. Activation of the adenosine A3 receptor in RAW 264.7 cells inhibits lipopolysaccharide-stimulated tumor necrosis factor-alpha release by reducing calcium-dependent activation of nuclear factor-kappaB and extracellular signal-regulated kinase 1/2. *J. Pharmacol. Exp. Ther.* **316:** 71–78.
16. Jeong, H. J., S. H. Hong, R. K. Park, N. H. An, and H. M. Kim. 2005. Ethanol induces the production of cytokines via the Ca2+, MAP kinase, HIF-1alpha, and NF-kappaB pathway. *Life Sci.* **77:** 2179–2192.
17. Gewirtz, A. T., A. S. Rao, P. O. Simon, Jr., D. Merlin, D. Carnes, J. L. Madara, and A. S. Neish. 2000. Salmonella typhimurium induces epithelial IL-8 expression via Ca(2+)-mediated activation of the NF-kappaB pathway. *J. Clin. Invest.* **105:** 79–92.
18. Melien, O., L. S. Nilssen, O. F. Dajani, K. L. Sand, J. G. Iversen, D. L. Sandnes, and T. Christoffersen. 2002. Ca2+-mediated activation of ERK in hepatocytes by norepinephrine and prostaglandin F2 alpha: role of calmodulin and Src kinases. *BMC Cell Biol.* **3:** 5.
19. Balsinde, J., H. Shinohara, L. J. Lefkowitz, C. A. Johnson, M. A. Balboa, and E. A. Dennis. 1999. Group V phospholipase A(2)-dependent induction of cyclooxygenase-2 in macrophages. *J. Biol. Chem.* **274:** 25967–25970.
20. Qiu, Z. H., M. S. de Carvalho, and C. C. Leslie. 1993. Regulation of phospholipase A2 activation by phosphorylation in mouse peritoneal macrophages. *J. Biol. Chem.* **268:** 24506–24513.
21. Means, A. R. 2000. Regulatory cascades involving calmodulin-dependent protein kinases. *Mol. Endocrinol.* **14:** 4–13.
22. Colomer, J., and A. R. Means. 2007. Physiological roles of the Ca2+/CaM-dependent protein kinase cascade in health and disease. *Subcell. Biochem.* **45:** 169–214.

23. Miller, C. W., D. A. Casimir, and J. M. Ntambi. 1996. The mechanism of inhibition of 3T3–L1 preadipocyte differentiation by prostaglandin F2alpha. *Endocrinology.* **137:** 5641–5650.

24. Thastrup, O., J. P. Cullen, B. K. Drobak, M. R. Hanley, and A. P. Dawson. 1990. Thapsigargin, a tumor promoter, discharges intracellular Ca2+ stores by specific inhibition of the endoplasmic reticulum Ca2(+)-ATPase. *Proc. Natl. Acad. Sci. USA.* **87:** 2466–2470.

25. LaRosa, P. C., J. J. Riethoven, H. Chen, Y. Xia, Y. Zhou, M. Chen, J. Miner, and M. E. Fromm. 2007. Trans-10, cis-12 conjugated linoleic acid activates the integrated stress response pathway in adipocytes. *Physiol. Genomics.* **31:** 544–553.

26. Camina, J. P., X. Casabiell, and F. F. Casanueva. 1999. Inositol 1,4,5-trisphosphate-independent Ca2+ mobilization triggered by a lipid factor isolated from vitreous body. *J. Biol. Chem.* **274:** 28134–28141.

27. Pahl, H. L., and P. A. Baeuerle. 1996. Activation of NF-kappa B by ER stress requires both Ca2+ and reactive oxygen intermediates as messengers. *FEBS Lett.* **392:** 129–136.

28. Tokumitsu, H., T. Chijiwa, M. Hagiwara, A. Mizutani, M. Terasawa, and H. Hidaka. 1990. KN-62, 1-[N,O-bis(5-isoquinolinesulfonyl)-N-methyl-L-tyrosyl]-4-phenylpiperazi ne, a specific inhibitor of Ca2+/calmodulin-dependent protein kinase II. *J. Biol. Chem.* **265:** 4315–4320.

29. Tornquist, K., and E. Ekokoski. 1996. Inhibition of agonist-mediated calcium entry by calmodulin antagonists and by the Ca2+/calmodulin kinase II inhibitor KN-62. Studies with thyroid FRTL-5 cells. *J. Endocrinol.* **148:** 131–138.

30. Cui, Z. J., H. Hidaka, and P. S. Dannies. 1996. KN-62, a calcium/calmodulin-dependent protein kinase II inhibitor, inhibits high potassium-stimulated prolactin secretion and intracellular calcium increases in anterior pituitary cells. *Biochim. Biophys. Acta.* **1310:** 343–347.

31. Marley, P. D., and K. A. Thomson. 1996. The Ca++/calmodulin-dependent protein kinase II inhibitors KN62 and KN93, and their inactive analogues KN04 and KN92, inhibit nicotinic activation of tyrosine hydroxylase in bovine chromaffin cells. *Biochem. Biophys. Res. Commun.* **221:** 15–18.

32. Suh, H. N., H. T. Huong, C. H. Song, J. H. Lee, and H. J. Han. 2008. Linoleic acid stimulates gluconeogenesis via Ca2+/PLC, cPLA2, and PPARs pathways through GPR40 in primary cultured chicken hepatocytes. *Am. .J Physiol. Cell Physiol.* **295:** C1518–C1527.

33. Andrei, C., P. Margiocco, A. Poggi, L. V. Lotti, M. R. Torrisi, and A. Rubartelli. 2004. Phospholipases C and A2 control lysosome-mediated IL-1 beta secretion: implications for inflammatory processes. *Proc. Natl. Acad. Sci. USA.* **101:** 9745–9750.

34. Butow, R. A., and N. G. Avadhani. 2004. Mitochondrial signaling: the retrograde response. *Mol. Cell.* **14:** 1–15.

35. Luo, Y., J. D. Bond, and V. M. Ingram. 1997. Compromised mitochondrial function leads to increased cytosolic calcium and to activation of MAP kinases. *Proc. Natl. Acad. Sci. USA.* **94:** 9705–9710.

36. Arnould, T., S. Vankoningsloo, P. Renard, A. Houbion, N. Ninane, C. Demazy, J. Remacle, and M. Raes. 2002. CREB activation induced by mitochondrial dysfunction is a new signaling pathway that impairs cell proliferation. *EMBO J.* **21:** 53–63.

37. Borodinsky, L. N., O. A. Coso, and M. L. Fiszman. 2002. Contribution of Ca2+ calmodulin-dependent protein kinase II and mitogen-activated protein kinase kinase to neural activity-induced neurite outgrowth and survival of cerebellar granule cells. *J. Neurochem.* **80:** 1062–1070.

38. Ginnan, R., P. J. Pfleiderer, K. Pumiglia, and H. A. Singer. 2004. PKC-delta and CaMKII-delta 2 mediate ATP-dependent activation of ERK1/2 in vascular smooth muscle. *Am. J. Physiol. Cell Physiol.* **286:** C1281–C1289.

39. Huang, S. H., W. J. Shen, H. L. Yeo, and S. M. Wang. 2004. Signaling pathway of magnolol-stimulated lipolysis in sterol ester-loaded 3T3–L1 preadipocyes. *J. Cell. Biochem.* **91:** 1021–1029.

40. Lu, K. K., S. E. Armstrong, R. Ginnan, and H. A. Singer. 2005. Adhesion-dependent activation of CaMKII and regulation of ERK activation in vascular smooth muscle. *Am. J. Physiol. Cell Physiol.* **289:** C1343–C1350.

41. Montiel, M., J. Quesada, and E. Jimenez. 2007. Activation of calcium-dependent kinases and epidermal growth factor receptor regulate muscarinic acetylcholine receptor-mediated MAPK/ERK activation in thyroid epithelial cells. *Cell. Signal.* **19:** 2138–2146.

42. Cuschieri, J., E. Bulger, I. Garcia, S. Jelacic, and R. V. Maier. 2005. Calcium/calmodulin-dependent kinase II is required for platelet-activating factor priming. *Shock.* **23:** 99–106.

43. Draznin, B., K. Sussman, M. Kao, D. Lewis, and N. Sherman. 1987. The existence of an optimal range of cytosolic free calcium for insulin-stimulated glucose transport in rat adipocytes. *J. Biol. Chem.* **262:** 14385–14388.

44. Draznin, B., K. E. Sussman, R. H. Eckel, M. Kao, T. Yost, and N. A. Sherman. 1988. Possible role of cytosolic free calcium concentrations in mediating insulin resistance of obesity and hyperinsulinemia. *J. Clin. Invest.* **82:** 1848–1852.

45. Begum, N., W. Leitner, J. E. Reusch, K. E. Sussman, and B. Draznin. 1993. GLUT-4 phosphorylation and its intrinsic activity. Mechanism of Ca(2+)-induced inhibition of insulin-stimulated glucose transport. *J. Biol. Chem.* **268:** 3352–3356.

46. Draznin, B., D. Lewis, N. Houlder, N. Sherman, M. Adamo, W. T. Garvey, D. LeRoith, and K. Sussman. 1989. Mechanism of insulin resistance induced by sustained levels of cytosolic free calcium in rat adipocytes. *Endocrinology.* **125:** 2341–2349.

47. Jang, Y. J., H. J. Ryu, Y. O. Choi, C. Kim, C. H. Leem, and C. S. Park. 2002. Improvement of insulin sensitivity by chelation of intracellular Ca(2+) in high-fat-fed rats. *Metabolism.* **51:** 912–918.

48. Ou, L., Y. Wu, C. Ip, X. Meng, Y. C. Hsu, and M. M. Ip. 2008. Apoptosis induced by t10,c12-conjugated linoleic acid is mediated by an atypical endoplasmic reticulum stress response. *J. Lipid Res.* **49:** 985–994.